NANO LETTERS

Letter

pubs.acs.org/NanoLett

Polysulfide-Blocking Microporous Polymer Membrane Tailored for Hybrid Li-Sulfur Flow Batteries

Changyi Li,[†,‡,§] Ashleigh L. Ward,[†,‡] Sean E. Doris,[†,‡,∥] Tod A. Pascal,[‡] David Prendergast,[‡] and Brett A. Helms*[,†,‡]

[†]The Joint Center for Energy Storage Research, 1 Cyclotron Road, Berkeley, California 94720, United States

[‡]The Molecular Foundry, Lawrence Berkeley National Laboratory, 1 Cyclotron Road, Berkeley, California 94720, United States

[§]Department of Chemical and Biomolecular Engineering, University of California, Berkeley, California 94720, United States

[∥]Department of Chemistry, University of California, Berkeley, California 94720, United States

Supporting Information

ABSTRACT: Redox flow batteries (RFBs) present unique opportunities for multi-hour electrochemical energy storage (EES) at low cost. Too often, the barrier for implementing them in large-scale EES is the unfettered migration of redox active species across the membrane, which shortens battery life and reduces Coulombic efficiency. To advance RFBs for reliable EES, a new paradigm for controlling membrane transport selectivity is needed. We show here that size- and ion-selective transport can be achieved using membranes fabricated from polymers of intrinsic microporosity (PIMs). As a proof-of-concept demonstration, a first-generation PIM membrane dramatically reduced polysulfide crossover (and shuttling at the anode) in lithium−sulfur batteries, even when sulfur cathodes were prepared as flowable energy-dense fluids. The design of our membrane platform was informed by molecular dynamics simulations of the solvated structures of lithium bis(trifluoromethanesulfonyl)imide (LiTFSI) vs lithiated polysulfides (Li_2S_x, where x = 8, 6, and 4) in glyme-based electrolytes of different oligomer length. These simulations suggested polymer films with pore dimensions less than 1.2−1.7 nm might incur the desired ion-selectivity. Indeed, the polysulfide blocking ability of the PIM-1 membrane (~0.8 nm pores) was improved 500-fold over mesoporous Celgard separators (~17 nm pores). As a result, significantly improved battery performance was demonstrated, even in the absence of $LiNO_3$ anode-protecting additives.

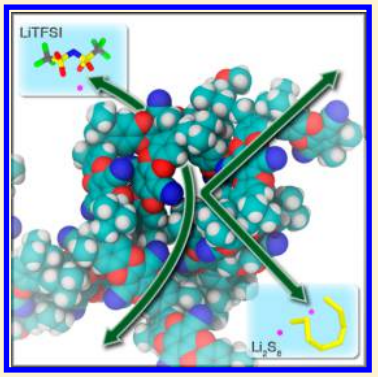

KEYWORDS: *Polymers of intrinsic microporosity, ion-selective membrane, size-selective membrane, electrochemical energy storage, redox flow battery, lithium−sulfur battery*

Membranes (or separators) are critical for ionic conduction and electronic isolation in many electrochemical devices. For cell architectures that utilize redox-active species that are dissolved, dispersed, or suspended in electrolyte, from fuel cells[1−3] (FCs) to redox flow batteries[4−11] (RFBs), it is also imperative that the membrane prevent active material crossover that would otherwise contribute to device shorting, electrode fouling, or irrevokable loss in capacity. Unfortunately, commercial battery separators, which feature shape-persistent mesopores, are freely permeable to most active materials used in RFBs.[12] Alternative membrane separators have thus far relied heavily on variants of aqueous single-ion conductors, e.g., Nafion,[13−15] which may ultimately restrict the use of certain types of flowable electrodes. Considerably less attention has been paid to size-sieving as a mechanism to achieve membrane selectivity, although success in this regard would allow greater flexibility in battery chemistries. Despite the wide availability of porous materials[16] that might serve effectively as membrane components, including zeolites,[17] metal−organic frameworks,[18−20] covalent organic frameworks,[21] carbon nanotubes,[22−24] cyclic peptide nanotubes,[25−27] and microporous polymers,[28,29] rational design rules for achieving ion-selective transport via sieving in flow battery membranes have not been established.

Guided by theoretical calculations, we apply here polymers of intrinsic microporosity (PIMs) as a membrane platform for achieving high-flux, ion-selective transport in nonaqueous electrolytes. These polymers are synthesized in a single step and easily cast into large-area sheets with well-controlled pore structure and pore chemistry (Figure 1).[30−34] The unique micropore architecture of PIMs arises primarily from two molecular characteristics: (1) PIMs do not feature rotating bonds along their backbone; and (2) they incorporate rigid sharp bends into at least one of the constituent monomers at regular intervals along the polymer chain. Both features contribute to frustrated packing of polymer chains in the solid state.[35] As a result, PIMs are amorphous yet exhibit high intrinsic microporosity (<2 nm) and high surface area (300−1500 $m^2\ g^{-1}$).[36−38] The open pore architecture of PIMs suggested to us that they might be uniquely

Received: April 15, 2015
Revised: July 20, 2015
Published: August 3, 2015

DOI: 10.1021/acs.nanolett.5b02078
Nano Lett. 2015, 15, 5724−5729

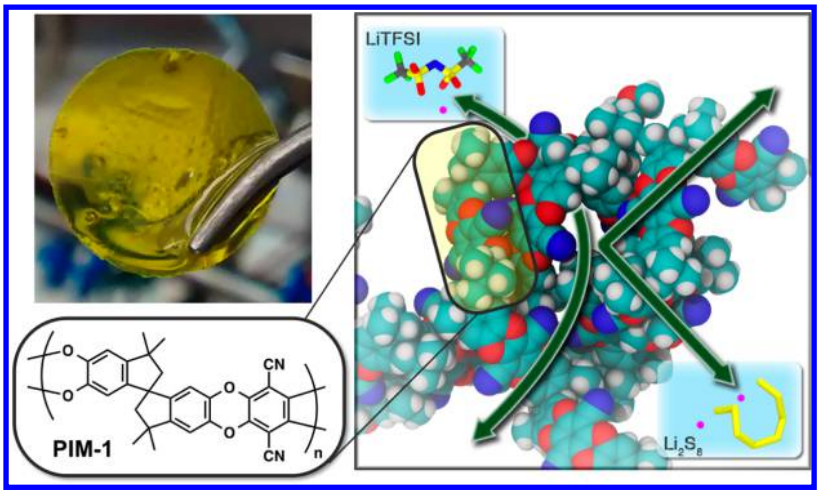

Figure 1. Ion-selective transport across membranes fabricated from PIM-1. For Li−S batteries, both stationary and hybrid flow, blocking Li_2S_x (where $x \geq 4$) crossover is critical to sustaining peak battery performance. We show that membranes based on PIM-1 achieve high transport selectivity for LiTFSI by reducing the membrane pore dimensions to subnanometer regimes, which shuts down polysulfide crossover via a sieving mechanism. Ion flux across the membrane is tied to overall microporosity, pore architecture, and electrolyte formulation.

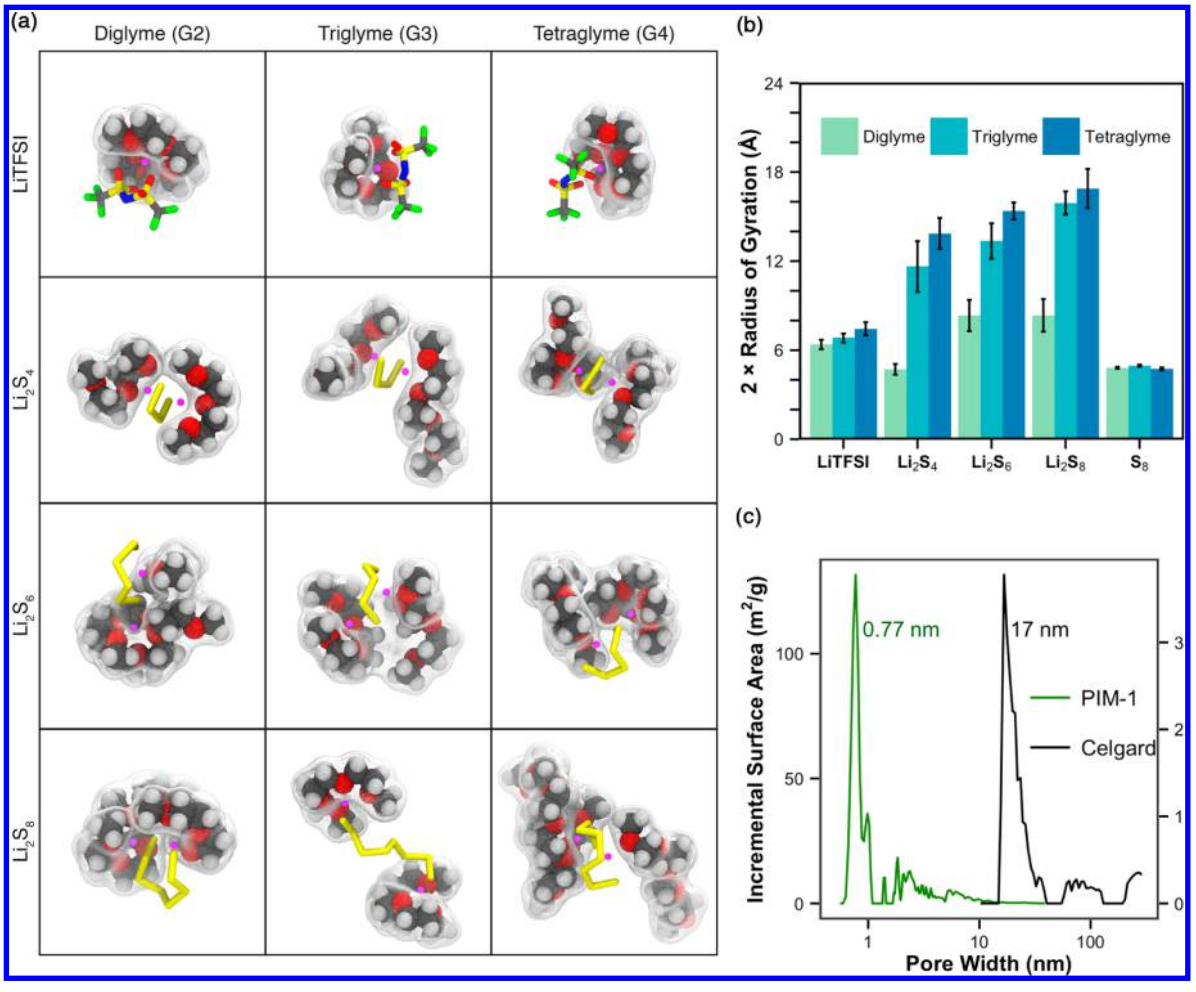

Figure 2. (a) Snapshots from MD simulations nearest to the average size of solvated LiTFSI and Li_2S_x (x = 4, 6, and 8) in diglyme, triglyme, and tetraglyme. (b) Calculated radii of gyration (R_g) for Li_2S_4, Li_2S_6, and Li_2S_8, along with their first solvation shells, in diglyme, triglyme, and tetraglyme as determined by MD simulations. (c) Pore size distributions for microporous PIM-1 vs mesoporous Celgard polymer membranes.

positioned for selective species transport in electrochemical devices via sieving.

We highlight here new opportunities for PIMs to serve as ion-selective membranes in RFBs,[39−45] using lithium−sulfur (Li−S) as a model battery chemistry. Here the lithium anode is stationary and separated, by the membrane, from the flowable sulfur-containing catholyte.[46,47] This RFB features a high theoretical specific energy capacity of 1670 mAh g^{-1} for S and

DOI: 10.1021/acs.nanolett.5b02078
Nano Lett. 2015, 15, 5724−5729

operating voltage that exceeds 2.0 V.[48−55] While these are desirable characteristics, this battery chemistry suffers from low Coulombic efficiency and rapid capacity fade when lithium polysulfides (PS) crossover to and react with the metal anode surface. Strategies seeking to mitigate PS crossover in Li−S batteries have included the use of sacrificial anode-protecting additives (e.g., $LiNO_3$),[56−59] single-ion conducting membranes,[13,14] conductive interlayers,[59−61] permselective barriers,[62] and even polysulfide adsorbates.[63−67] Nonetheless, continuous Li consumption upon cycling remains a problem. Our demonstration here that PIM membranes block PS crossover while allowing ions in the supporting electrolyte to traverse the membrane with minimal impedance indicates a direct solution to the PS crossover problem is feasible; we also show dramatically improved battery performance when PIM membranes are in place, rather than conventional battery separators.

To inform the rational design of a membrane platform capable of achieving high transport selectivity for supporting electrolyte (lithium bis(trifluoromethane)sulfonimide, LiTFSI) vs PS in Li−S RFBs, we carried out molecular dynamics (MD) simulations of each species' solvated structures in different ethereal solvents, diglyme (G2), triglyme (G3), and tetraglyme (G4), as these are commonly used in Li−S RFBs.[68−70] The simulated effective sizes of these solvated complexes were determined by the radii of gyration (R_g) of the solute and the first solvation shell. These shells were typically composed of two solvent molecules, as exemplified by the average snapshots shown in Figure 2a. We also calculated the size of elemental sulfur, which exhibits no explicit solvent coordination in our simulations. For this singular case, we determined a size for S_8 using its atoms' van der Waals solvent-excluded radii. Our determinations of R_g provide size-ranges for selective ion transport (Figure 2b). As the primary contributors to the shuttling currents are lithium polysulfides Li_2S_x where $x \geq 4$, the membrane pore dimensions should be smaller than 1.2−1.7 nm in order to achieve ion-selective transport.

Directed by our MD simulations, we identified PIM-1[30] as a possible PS-blocking membrane material for Li−S hybrid flow cells. PIM-1 is the progenitor of a family of non-networked ladder polymers that are mechanically[71] and thermally[72] robust; pertinent to their use here, their pore dimensions are sub-nm. PIM-1 was synthesized (200 kg mol^{-1}) on a multigram scale from inexpensive, commercially available monomers and cast from solution into flexible free-standing membranes (~10 μm thick) (Figures 1 and S1). We determined the specific surface area (795 m^2 g^{-1}) and pore size distribution of PIM-1 using nitrogen adsorption isotherms (Figure 2c). PIM-1 membranes had a nominal pore size of 0.77 nm, which is ideal for selective transport of LiTFSI and PS blocking. This stands in stark contrast with commercially available Celgard 2325, which has a much larger pore size of 17 nm: far too large for size-selective transport (Figure 2c). Celgard 2325 and similar mesoporous polymer separators[12] are commonly used in Li−S cells and serve as a useful benchmark for new membrane materials.[46] A total porosity of ~25% was determined for PIM-1 membranes using ellipsometric porosimetry, which is comparable to the porosity of Celgard 2325. As PIM-1 membranes are expected to swell to a degree upon introduction of electrolyte, this determination should be considered a lower limit to the available free volume.

We hypothesized that during battery operation the free volume in PIM-1 (and PIMs generally) would become swollen and infiltrated with electrolyte, creating an ionically percolating solution-phase conductive network. As a result, ion flux would be solely carried by (and be dependent on) the solution conductivity within the pores; polymer chain dynamics, which are orders of magnitude slower, would no longer dictate the membrane's ionic conductivity. To test this hypothesis, we evaluated PIM-1's membrane ionic conductivities in glymes of different oligomer lengths, diglyme (G2), triglyme (G3), and tetraglyme (G4), containing 0.50 M LiTFSI. We noted a strong correlation between the membrane ionic conductivity and the bulk solution ionic conductivity[73] of the electrolyte (Figure 3a).

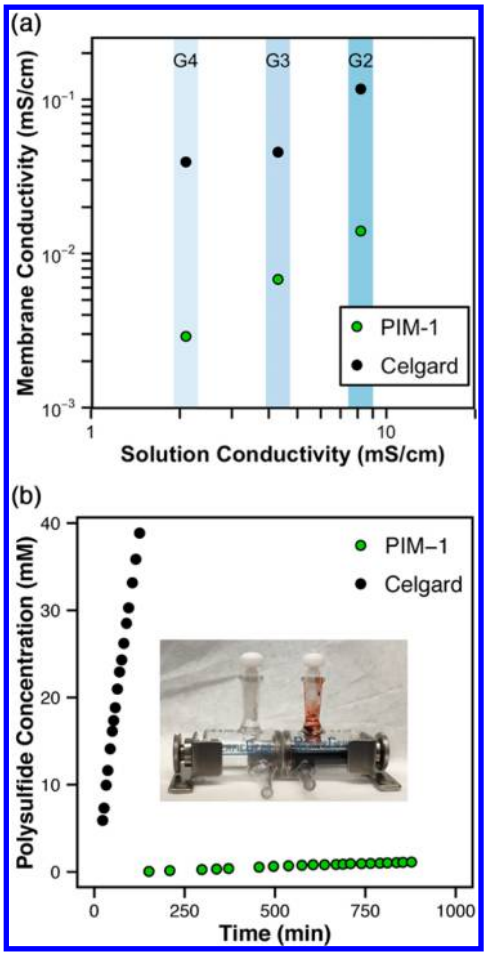

Figure 3. (a) Ambient temperature ionic conductivity of microporous PIM-1 vs mesoporous Celgard membranes infiltrated with different electrolyte formulations: 0.50 M LiTFSI in diglyme (G2), triglyme (G3), or tetraglyme (G4). (b) Time-evolution of the concentration of PS in the permeate (left) of H-cells configured with either a Celgard (black) or a PIM-1 (green) membrane. The retentate was charged with an initial concentration of 2.5 M S as Li_2S_8 in diglyme containing 0.50 M LiTFSI and 0.15 M $LiNO_3$. The concentration of PS in the permeate was determined electrochemically.

These results indicate that the ion current is indeed carried by the infiltrating electrolyte, as predicted. This behavior was also observed in Celgard separators (Figure 3a). By comparing the membrane ionic conductivities for Celgard and PIM-1, we found that reducing the pore dimensions from 17 to 0.77 nm, respectively, only decreased membrane ionic conductivity 10-fold. We also found that electrolytes based on diglyme provided the highest membrane ionic conductivity for both platforms and was thus chosen as the supporting electrolyte for all subsequent experiments.

To quantify the polysulfide-blocking ability of PIM-1 vs Celgard, we performed membrane crossover experiments in

DOI: 10.1021/acs.nanolett.5b02078
Nano Lett. 2015, 15, 5724−5729

H-cells configured with dissolved PS (2.5 M S as Li_2S_8 in diglyme containing 0.50 M LiTFSI and 0.15 M $LiNO_3$) on the retentate side and PS-free electrolyte on the permeate side (Figure 3b, inset). The concentration of PS over time was then monitored electrochemically on the permeate side using either cyclic voltammetry or square wave voltammetry, where current could be correlated to concentration of PS via a calibration curve (Figures S2 and S3). Using an initial rate approximation, the diffusion coefficient of PS across the membranes were calculated to be 6.8×10^{-8} cm^2 s^{-1} for Celgard and 1.3×10^{-10} cm^2 s^{-1} for PIM-1 (~500-fold reduction). This is compelling evidence that PS are screened by a size-sieving mechanism within PIM-1's ionically percolating micropore network, as hypothesized. This PS-blocking ability comes at minimal expense to overall membrane ionic conductivity compared to Celgard, thus highlighting the value in guiding membrane design through careful examination of the solvated structures of ions vs redox active species in the electrolyte.

Given the outstanding PS-blocking ability of the PIM-1 membrane, their performance in Li−S batteries was tested employing soluble sulfur catholytes. To do so, Swagelok cells were assembled with Li-metal anodes, polysulfide catholytes (2.5 M S as Li_2S_8 in diglyme containing 0.50 M LiTFSI), and Celgard or PIM-1 membranes. Lithium anodes were scraped to reveal a fresh surface prior to cell assembly. Seeking to isolate the membrane's influence on mitigating PS shuttling currents, $LiNO_3$ additives were deliberately avoided in the electrolyte formulation. Moreover, to improve sulfur utilization, 5 wt % Ketjenblack was employed as an embedded current collector in the catholyte.[42,46] Three break-in cycles at C/10 were used to equilibrate PIM-1's membrane microenvironments before cycling at a C/8 rate. Overall, higher capacity fade was observed for both types of cells during the break-in due to the ample time allowed for polysulfide shuttling. The Li−S cells configured with Celgard membranes exhibited a drastic capacity fade from ~150 Wh L^{-1} after the break-in cycles to less than 20 Wh L^{-1} within the first 20 cycles, all at a C/8 rate. In contrast, batteries configured with PIM-1 membranes exhibited higher capacity at all cycles, sustaining 50 Wh L^{-1} at the end of 50 cycles (Figure 4a). The performance of PIM-1 membranes was further improved with the addition of $LiNO_3$ as an anode-protecting additive, with a sustained capacity of approximately 100 Wh L^{-1} after 50 cycles (Figure 4a) and stable cycling at rates as high as C/4 (Figure 4b). These results represent improvements in capacity retention over related work with Li−S flow cells, particularly in the absence of $LiNO_3$, and highlight the possibility for combining our membrane approach with other strategies to mitigate the effects of polysulfide crossover.[59,74]

Conclusion. Redox flow batteries present unique opportunities for low-cost, multi-hour energy storage, but also limitations. In order for RFBs to mature as a deployable technology, their longevity should be greatly improved for battery chemistries offering high-power performance. Toward that end, we highlighted the transport needs for membranes employed in nonaqueous Li−S cells, where the cathode was formulated as an energy-dense, flowable solution of polysulfides with Ketjenblack as an embedded current collector. We showed that rational principles for membrane design emerge from molecular dynamics simulations of the solvated structures of S_8, Li_2S_x (x = 8, 6, or 4), and LiTFSI in different electrolytes, and more specifically, that their calculated radius of gyration places an upper limit of 1.2−1.7 nm on the pore dimensions required for polysulfide blocking. Indeed, we showed that membranes processed from polymers of intrinsic microporosity exhibited unprecedented blocking characteristics for soluble polysulfides owing to their sub-nm pore dimensions. This blocking ability led to significantly improved device performance with respect to capacity fade and other important metrics. Given that the pore size, pore chemistry, and overall porosity for PIM membranes are tunable using molecular engineering and polymer processing, the membrane's transport characteristics can be tailored to suit a broad spectrum of electrochemical devices, including stationary batteries and fuel cells. Our success suggests a revolution in ion-transporting membranes is within reach.

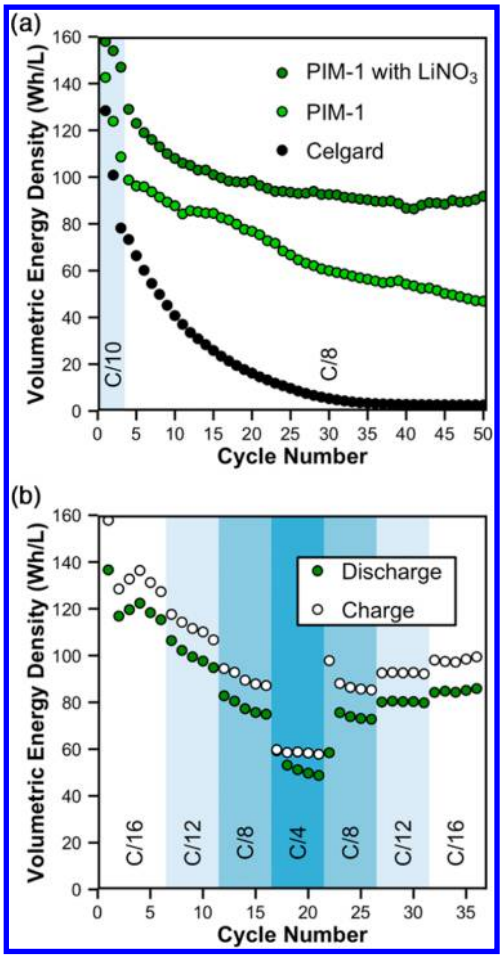

Figure 4. (a) Volumetric energy density as a function of cycle number for Celgard membrane with no $LiNO_3$ (black circles), PIM-1 membrane with no $LiNO_3$ (light green circles), and PIM-1 membrane with $LiNO_3$ additive (dark green circles). (b) Rate performance of PIM-1 membrane with $LiNO_3$ additive.

■ ASSOCIATED CONTENT

Supporting Information

The Supporting Information is available free of charge on the ACS Publications website at DOI: 10.1021/acs.nanolett.5b02078.

Detailed synthetic procedures, computational methods, electroanalytical methods, battery cycling data, and Supporting Figures S1−S8 (PDF)

■ AUTHOR INFORMATION

Corresponding Author

*E-mail:bahelms@lbl.gov.

DOI: 10.1021/acs.nanolett.5b02078
Nano Lett. 2015, 15, 5724−5729

Notes

The authors declare no competing financial interest.

■ ACKNOWLEDGMENTS

We thank D. Sun for assistance with nitrogen adsorption experiments, A. Bondaz for assistance with ellipsometric porosimetry. E. Wong, S. Ferreira, P. Chavez, B. Smith, and D. Li for electrode fabrication, and P. Frischmann and L. C. H. Gerber for helpful discussions. C.L., A.L.W., and B.A.H. were supported by the Joint Center for Energy Storage Research, an Energy Innovation Hub funded by the U.S. Department of Energy, Office of Science, Office of Basic Energy Sciences. S.E.D. was supported by the Department of Defense through the National Defense Science & Engineering Graduate Fellowship program. D.P. and T.A.P. acknowledge support from the Batteries for Advanced Transportation Technologies program, administered by the Assistant Secretary for Energy Efficiency and Renewable Energy, Office of Vehicle Technologies of the U.S. Department of Energy under Contract DE-AC02-05CH11231. Portions of the work, including polymer synthesis and characterization, molecular dynamics simulations, polymer processing, membrane crossover experiments, and Li−S battery performance, were carried out as User Projects at the Molecular Foundry, which is supported by the Office of Science, Office of Basic Energy Sciences, of the U.S. Department of Energy under Contract No. DE-AC02-05CH11231. The computational portion of this work used resources of the National Energy Research Scientific Computing Center, a DOE Office of Science User Facility supported by the Office of Science of the U.S. Department of Energy under the same contract.

■ REFERENCES

(1) Steele, B. C. H.; Heinzel, A. *Nature* **2001**, *414*, 345−532.
(2) Kerres, J. A. *J. Membr. Sci.* **2001**, *185*, 3−27.
(3) Borup, R.; Meyers, J.; Pivovar, B.; Kim, Y. S.; Mukundan, R.; Garland, N.; Myers, D.; Wilson, M.; Garzon, F.; Wood, D.; Zelenay, P.; More, K.; Stroh, K.; Zawodzinski, T.; Boncella, J.; McGrath, J. E.; Inaba, M.; Miyatake, K.; Hori, M.; Ota, K.; Ogumi, Z.; Nishikata, A.; Siroma, Z.; Uchimoto, Y.; Yasuda, K.; Kimijima, K.; Iwashita, N. *Chem. Rev.* **2007**, *107*, 3904−3951.
(4) Skyllas-Kazacos, M.; Rychcik, M.; Robins, R. G.; Fane, A. G.; Green, M. A. *J. Electrochem. Soc.* **1986**, *133*, 1057−1058.
(5) Lopez-Atalaya, M.; Codina, G.; Perez, J. R.; Vazquez, J. L.; Aldaz, A. *J. Power Sources* **1992**, *39*, 147−154.
(6) Fabjan, C.; Garche, J.; Harrer, B.; Jörissen, L.; Kolbeck, C.; Philippi, F.; Tomazic, G.; Wagner, F. *Electrochim. Acta* **2001**, *47*, 825−831.
(7) Joerissen, L.; Garche, J.; Fabjan, C.; Tomazic, G. *J. Power Sources* **2004**, *127*, 98−104.
(8) Weber, A. Z.; Mench, M. M.; Meyers, J. P.; Ross, P. N.; Gostick, J. T.; Liu, Q. *J. Appl. Electrochem.* **2011**, *41*, 1137−1164.
(9) Dunn, B.; Kamath, H.; Tarascon, J.-M. *Science* **2011**, *334*, 928−935.
(10) Wang, W.; Luo, Q.; Li, B.; Wei, X.; Li, L.; Yang, Z. *Adv. Funct. Mater.* **2013**, *23*, 970−986.
(11) Huang, Q.; Wang, Q. *ChemPlusChem* **2015**, *80*, 312−322.
(12) Arora, P.; Zhang, Z. *Chem. Rev.* **2004**, *104*, 4419−4462.
(13) Huang, J.; Zhang, Q.; Peng, H.; Chen, C.; Wei, F. *Energy Environ. Sci.* **2014**, *7*, 347−353.
(14) Bauer, I.; Thieme, S.; Bruckner, J.; Althues, H.; Kaskel, S. *J. Power Sources* **2014**, *251*, 417−422.
(15) Jin, Z.; Xie, K.; Hong, X.; Hu, Z.; Liu, X. *J. Power Sources* **2012**, *218*, 163−167.
(16) Thomas, A. *Angew. Chem., Int. Ed.* **2010**, *49*, 8328−8344.
(17) Caro, J.; Noack, M. *Microporous Mesoporous Mater.* **2008**, *115*, 215−233.
(18) Yaghi, O. M.; O'Keeffe, M.; Ockwig, N. W.; Chae, H. K.; Eddaoudi, M.; Kim, J. *Nature* **1999**, *402*, 276−279.
(19) Kitagawa, S.; Kitaura, R.; Noro, S. *Angew. Chem., Int. Ed.* **2004**, *43*, 2334−2375.
(20) Chung, T.-S.; Jiang, L. Y.; Li, Y.; Kulprathipanja, S. *Prog. Polym. Sci.* **2007**, *32*, 483−507.
(21) Colson, J. W.; Dichtel, W. R. *Nat. Chem.* **2013**, *5*, 453−465.
(22) Martin, C. R.; Lakshmi, B. B.; Fisher, E. R.; Che, G. *Nature* **1998**, *393*, 346−349.
(23) Hinds, B. J.; Chopra, N.; Rantell, T.; Andrews, R.; Gavalas, V.; Bachas, L. G. *Science* **2004**, *303*, 62−65.
(24) Geng, J.; Kim, K.; Zhang, J.; Escalada, A.; Tunuguntla, R.; Comolli, L. R.; Allen, F. I.; Shnyrova, A. V.; Cho, K. R.; Munoz, D.; Wang, Y. M.; Grigoropoulos, C. P.; Ajo-Franklin, C. M.; Frolov, V. A.; Noy, A. *Nature* **2014**, *514*, 612−615.
(25) Ghadiri, M. R.; Granja, J. R.; Buehler, L. K. *Nature* **1994**, *369*, 301−304.
(26) Xu, T.; Zhao, N.; Ren, F.; Hourani, R.; Lee, M. T.; Shu, J. Y.; Mao, S.; Helms, B. A. *ACS Nano* **2011**, *5*, 1376−1384.
(27) Hourani, R.; Zhang, C.; van der Weegen, R.; Ruiz, L.; Li, C.; Keten, S.; Helms, B. A.; Xu, T. *J. Am. Chem. Soc.* **2011**, *133*, 15296−15299.
(28) McKeown, N. B.; Budd, P. M. *Chem. Soc. Rev.* **2006**, *35*, 675−683.
(29) Budd, P. M.; McKeown, N. B. *Polym. Chem.* **2010**, *1*, 63−68.
(30) Budd, P. M.; Ghanem, B. S.; Makhseed, S.; McKeown, N. B.; Msayib, K. J.; Tattershall, C. E. *Chem. Commun.* **2004**, 230−231.
(31) Budd, P. M.; Msayib, K. J.; Tattershall, C. E.; Ghanem, B. S.; Reynolds, K. J.; McKeown, N. B.; Fritsch, D. *J. Membr. Sci.* **2005**, *251*, 263−269.
(32) Staiger, C. L.; Pas, S. J.; Hill, A. J.; Cornelius, C. J. *Chem. Mater.* **2008**, *20*, 2606−2608.
(33) McKeown, N. B.; Budd, P. M. *Macromolecules* **2010**, *43*, 5163−5176.
(34) Du, N.; Dal-Cin, M. M.; Pinnau, I.; Nicalek, A.; Robertson, G. P.; Guiver, M. D. *Macromol. Rapid Commun.* **2011**, *32*, 631−636.
(35) Heuchel, M.; Fritsch, D.; Budd, P. M.; McKeown, N. B.; Hofmann, D. *J. Membr. Sci.* **2008**, *318*, 84−99.
(36) Du, N.; Park, H. B.; Robertson, G. P.; Dal-Cin, M. M.; Visser, T.; Scoles, L.; Guiver, M. D. *Nat. Mater.* **2011**, *10*, 372−375.
(37) Carta, M.; Malpass-Evans, R.; Croad, M.; Rogan, Y.; Jansen, J. C.; Bernardo, P.; Bazzarelli, F.; McKeown, N. B. *Science* **2013**, *339*, 303−307.
(38) Shamsipur, H.; Dawood, B. A.; Budd, P. M.; Bernardo, P.; Clarizia, G.; Jansen, J. C. *Macromolecules* **2014**, *47*, 5595−5606.
(39) Li, X.; Zhang, H.; Mai, Z.; Zhang, H.; Vankelecom, I. *Energy Environ. Sci.* **2011**, *4*, 1147−1160.
(40) Gu, M.; Lee, J.; Kim, Y.; Kim, J. S.; Jang, B. Y.; Lee, K. T.; Kim, B.-S. *RSC Adv.* **2014**, *4*, 46940−46946.
(41) Liu, Q.; Sleightholme, A. E. S.; Shinkle, A. A.; Li, Y.; Thompson, L. T. *Electrochem. Commun.* **2009**, *11*, 2312−2315.
(42) Duduta, M.; Ho, B.; Wood, V. C.; Limthongkul, P.; Brunini, V. E.; Carter, W. C.; Chiang, Y.-M. *Adv. Energy Mater.* **2011**, *1*, 511−516.
(43) Leung, P.; Li, X.; Ponce de León, C.; Berlouis, L.; Low, C. T. J.; Walsh, F. C. *RSC Adv.* **2012**, *2*, 10125−10156.
(44) Shin, S.-H.; Yun, S.-H.; Moon, S.-H. *RSC Adv.* **2013**, *3*, 9095−9116.
(45) Huang, Q.; Li, H.; Grätzel, M.; Wang, Q. *Phys. Chem. Chem. Phys.* **2013**, *15*, 1793−1797.
(46) Fan, F. Y.; Woodford, W. H.; Li, Z.; Baram, N.; Smith, K. C.; Helal, A.; McKinley, G. H.; Carter, W. C.; Chiang, Y.-M. *Nano Lett.* **2014**, *14*, 2210−2218.
(47) Yang, Y.; Zheng, G.; Cui, Y. *Energy Environ. Sci.* **2013**, *6*, 1552−1558.
(48) Rauh, R. D.; Abraham, K. M.; Pearson, G. F.; Surprenant, J. K.; Brummer, S. B. *J. Electrochem. Soc.* **1979**, *126*, 523−527.
(49) Bruce, P. G.; Freunberger, S. A.; Hardwick, L. J.; Tarascon, J.-M. *Nat. Mater.* **2012**, *11*, 19−29.
(50) Cuisinier, M.; Cabelguen, P.-E.; Evers, S.; He, G.; Kolbeck, M.; Garsuch, A.; Bolin, T.; Balasubramanian, M.; Nazar, L. F. *J. Phys. Chem. Lett.* **2013**, *4*, 3227−3232.

DOI: 10.1021/acs.nanolett.5b02078
Nano Lett. 2015, 15, 5724−5729

(51) Barghamadi, M.; Kapoor, A.; Wen, C. *J. Electrochem. Soc.* **2013**, *160*, A1256−A1263.
(52) Assary, R. S.; Curtiss, L. A.; Moore, J. S. *J. Phys. Chem. C* **2014**, *118*, 11545−11558.
(53) Vijayakumar, M.; Govind, N.; Walter, E.; Burton, S. D.; Shukla, A.; Devaraj, A.; Xiao, J.; Liu, J.; Wang, C.; Karima, A.; Thevuthasana, S. *Phys. Chem. Chem. Phys.* **2014**, *16*, 10923−10932.
(54) Manthiram, A.; Fu, Y.; Chung, S.-H.; Zu, C.; Su, Y.-S. *Chem. Rev.* **2014**, *114*, 11751−11787.
(55) Wu, H.-L.; Huff, L. A.; Gewirth, A. A. *ACS Appl. Mater. Interfaces* **2015**, *7*, 1709−1719.
(56) Aurbach, D.; Pollak, E.; Elazari, R.; Salitra, G.; Kelley, C. S.; Affinito, J. *J. Electrochem. Soc.* **2009**, *156*, A694−A702.
(57) Zhang, S. S. *Electrochim. Acta* **2012**, *70*, 344−348.
(58) Rosenman, A.; Elazari, R.; Salitra, G.; Markevich, E.; Aurbach, D.; Garsuch, A. *J. Electrochem. Soc.* **2015**, *162*, A470−A473.
(59) Su, Y. S.; Manthiram, A. *Nat. Commun.* **2012**, *3*, 1166.
(60) Zhou, G.; Pei, S.; Li, L.; Wang, D.-W.; Wang, S.; Huang, K.; Yin, L.; Li, F.; Cheng, H.-M. *Adv. Mater.* **2014**, *26*, 625−631.
(61) Yao, H.; Yan, K.; Li, W.; Zheng, G.; Kong, D.; Seh, Z. W.; Narasimhan, V. K.; Liang, Z.; Cui, Y. *Energy Environ. Sci.* **2014**, *7*, 3381−3390.
(62) Huang, J.; Zhuang, T.; Zhang, Q.; Peng, H.; Chen, C.; Wei, F. *ACS Nano* **2015**, *9*, 3002−3011.
(63) Hart, C. J.; Cuisinier, M.; Liang, X.; Kundu, D.; Garsuch, A.; Nazar, L. F. *Chem. Commun.* **2015**, *51*, 2308−2311.
(64) Pang, Q.; Kundu, D.; Cuisinier, M.; Nazar, L. F. *Nat. Commun.* **2014**, *5*, 4759.
(65) Tao, X.; Wang, J.; Ying, Z.; Cai, Q.; Zheng, G.; Gan, Y.; Huang, H.; Xia, Y.; Liang, C.; Zhang, W.; Cui, Y. *Nano Lett.* **2014**, *14*, 5288−5294.
(66) Wang, Z.; Dong, Y.; Li, H.; Zhao, Z.; Bin Wu, H.; Hao, C.; Liu, S.; Qiu, J.; Lou, X. W. *Nat. Commun.* **2014**, *5*, 5002.
(67) Zhang, Q.; Wang, Y.; Seh, Z. W.; Fu, Z.; Zhang, R.; Cui, Y. *Nano Lett.* **2015**, *15*, 3780−3786.
(68) Henderson, W. A.; Brooks, N. R.; Young, V. G. *Chem. Mater.* **2003**, *15*, 4685−4690.
(69) Henderson, W. A.; McKenna, F.; Khan, M. A.; Brooks, N. R.; Young, V. G.; Frech, R. *Chem. Mater.* **2005**, *17*, 2284−2289.
(70) Pascal, T. A.; Wujcik, K. H.; Velasco-Velez, J.; Wu, C.; Teran, A. A.; Kapilashrami, M.; Cabana, J.; Guo, J.; Salmeron, M.; Balsara, N.; Prendergast, D. *J. Phys. Chem. Lett.* **2014**, *5*, 1547−1551.
(71) Song, J.; Du, N.; Dai, Y.; Robertson, G. P.; Guiver, M. D.; Thomas, S.; Pinnau, I. *Macromolecules* **2008**, *41*, 7411−7417.
(72) Budd, P. M.; Elabas, E. S.; Ghanem, B. S.; Makhseed, S.; McKeown, N. B.; Msayib, K. J.; Tattershall, C. E.; Wang, D. *Adv. Mater.* **2004**, *16*, 456−459.
(73) Choquette, Y.; Brisard, G.; Parent, M.; Brouillette, D.; Perron, G.; Desnoyers, J. E.; Armand, M.; Gravel, D.; Slougui, N. *J. Electrochem. Soc.* **1998**, *145*, 3500.
(74) Chen, H.; Zou, Q.; Liang, Z.; Liu, H.; Li, Q.; Lu, Y. *Nat. Commun.* **2015**, *6*, 5877.

DOI: 10.1021/acs.nanolett.5b02078
Nano Lett. 2015, 15, 5724−5729